Journal Name

ARTICLE

Resonance Raman detection of antioxidants using an iron oxide nanoparticle catalysed decolourisation assay

Received 00th January 20xx,
Accepted 00th January 20xx

DOI: 10.1039/x0xx00000x

www.rsc.org/

Pee-reviewed accepted author manuscript (AAM).

Sian Sloan-Dennison,[a] Neil. C. Shand[b], Duncan Graham[a] and Karen Faulds[a]

Nanozymes are metal nanoparticles with catalytic properties that can be used to oxidise peroxidase substrates giving a colorimetric response which can be detected using UV-vis, and recently, Raman spectroscopy. Due to their ease of synthesis and increased stability, nanozymes are being increasing investigated to replace conventional enzymes for the detection of biomolecules. Here we exploit the catalytic activity of iron oxide (Fe_2O_3) nanoparticles combined with the substrate 2,2- azinobis (3-ethyl-benzothiazoline-6-sulfonic acid) (ABTS) in a decolourisation assay for the detection of antioxidants. Fe_2O_3 nanoparticles were used to catalyse the oxidation of ABTS to its green radical cation which, upon the addition of an antioxidant, resulted in a decolourisation due to the reduction of the radical cation caused by the hydrogen donating antioxidant. The assay was applied for the detection of multiple antioxidants (glutathione, chlorogenic acid and ascorbic acid), and was followed by monitoring the resonance Raman scattering from the ABTS solution using a portable Raman system with 785 nm laser excitation. This novel assay has the potential to be optimised to detect antioxidant activity in body fluid with low limits of detection with the potential for point of use monitoring.

Introduction

Artificial enzymes have become an increasingly interesting area of research and various nanoparticles have been investigated and used to mimic the structure and function of natural enzymes. The term nanozyme applies to nanoparticles which exhibit enzyme-like characteristics and efforts are being made to exploit this behaviour due to their attractive qualities over natural enzymes such as cost, easy synthesis and stability in a variety of conditions.[1]

It has recently been reported that iron oxide (Fe_3O_4 and Fe_2O_3) nanoparticles can behave as nanozymes and can catalyse the oxidation of the peroxidase substrates 2,2- azinobis (3-ethyl-benzothiazoline-6-sulfonic acid) (ABTS) and 3,3',5,5'-tetramethylbenzidine (TMB) in the presence of hydrogen peroxide (H_2O_2), yielding a green radical cation ($ABTS^{\cdot}+$) or blue charge transfer complex (TMB CTC).[2,3] As the oxidation of the substrates require the decomposition of H_2O_2, which is catalysed by the iron oxide nanoparticles, H_2O_2 itself has been detected colourmetrically by monitoring the decrease in absorbance of the $ABTS^{\cdot}+$ at lower concentrations of H_2O_2, with a limit of detection of 2.5 $x10^{-7}$ mol L^{-1} being achieved.[4] Glucose has also been detected using iron oxide nanoparticles with TMB and ABTS by utilising the reaction between glucose oxidase and glucose. Glucose oxidase breaks down glucose to produce gluconic acid and H_2O_2 which in the presence of iron oxide nanoparticles promotes the oxidation of TMB or ABTS and the intensity of the colour change can be related to how much H_2O_2 is produced and in turn, the concentration of glucose originally present.[3,5]

In addition to detecting H_2O_2 and glucose, Fe_3O_4 nanoparticles have also been used to replace the enzyme horse radish peroxidase (HRP) in enzyme linked immunosorbent assays (ELISAs) by functionalising the Fe_3O_4 nanoparticles with antibodies.[2] The antibody functionalised Fe_3O_4 nanoparticles bind to a specific antigen and catalyse the oxidation of TMB, in the presence of H_2O_2. The intensity of the oxidised product can be measured using UV-vis spectroscopy and can be related to the concentration of antigen present. Many biomolecules have been detected using this method including the rotavirus [6] and cardiac troponin I for myocardial infraction.[2]

Antioxidant activity is a measure of a molecules intrinsic reactivity towards free radicals and reactive oxidative species. Several assays have been reported for the detection and estimation of this activity including the oxygen radical absorption capacity (ORAC) assay,[7] the ferric reducing ability of plasma (FRAP) assay [8] and an ABTS decolourisation assay.[9] In the two step ABTS decolourisation assay for the detection of antioxidants, the colourless ABTS is first oxidised

[a] *Centre for Molecular Nanometrology, Technology and Innovation Centre, University of Strathclyde, 99 George Street, Glasgow, UK*
[b] *DSTL, Porton Down, Salisbury UK,*

† Footnotes relating to the title and/or authors should appear here.
Electronic Supplementary Information (ESI) available: [details of any supplementary information available should be included here]. See DOI: 10.1039/x0xx00000x

to the green radical cation (ABTS·+) using a variety of different molecules including silver (Ag+) ion,[10] potassium persulfate,[11] metmyoglobin [10] and HRP.[12] The second step then detects the presence of the antioxidant, via the decolourisation of the green ABTS·+ to the colourless ABTS as it is reduced by the antioxidant. The reduced ABTS·+ is conventionally detected using UV-vis spectroscopy, by monitoring the decrease in absorbance at 735 nm as the concentrations of antioxidants increases.[10] This assay is generally favoured over other antioxidant detection assays due to being relatively inexpensive, easy to use, having a good stability in a variety of pH's and a fast reaction time.[13] A number of antioxidants can be detected using this method including glutathione which is an important antioxidant involved in protecting cells from oxidative stress.[14] Depletion of glutathione has also been correlated with a poor immune system leaving the body more susceptible to infection.[15] Recently, Ma *et al.* have reported the detection of glutathione via an ABTS decolourisation assay, using Fe_3O_4 NPs as the catalyst in the oxidation of ABTS. The decolourisation was monitored using UV-vis spectroscopy and a linear range of 3 µM to 30 µM was obtained.[16] Furthermore, the authors used the assay to detect the presence of glutathione in A549 cells, indicating the possibility of using the technique to detect antioxidant activity in complex matrixes.

Raman spectroscopy, a powerful technique which can provide important structural information, has also been used to identify and characterise the redox behaviour of ABTS in the presence of hydroxylamine silver nanoparticles. When small quantities of ABTS·+ were formed, they interacted with the metal surface and when analysed with a 785 nm laser excitation, produced a surface enhanced Raman scattering (SERS) spectrum of ABTS·+ allowing detection of ABTS down to 2 µM.[17] The authors then suggest that SERS could therefore be used to monitor the ABTS decolourisation assay for the detection of antioxidants however this was not demonstrated.

In the work reported here we investigate for the first time the catalytic activity of Fe_2O_3 nanoparticles, which have an increased stability over Fe_3O_4 nanoparticles, for the detection of antioxidants using an ABTS decolourisation assay with resonance Raman scattering (RRS) detection (schematic shown in Figure 1). We demonstrate that Fe_2O_3 nanoparticles can catalyse the oxidation of ABTS in the presence of H_2O_2 generating ABTS·+. The ABTS·+ can then be reduced by an antioxidant and the reduction monitored using RRS, replacing the conventional UV-vis detection method with a molecularly specific vibrational technique and lowering the limits of detection. The measurements were carried out using a handheld portable Raman spectrometer allowing potential development as a point of use assay.

Materials

$FeCl_2.4H_2O$, $FeCl_3.6H_2O$, ABTS, 30 % H_2O_2, reduced glutathione, chlorogenic acid and ascorbic acid were all purchased form Sigma Aldrich, UK.

Instrumentation

UV-vis measurements were all carried out using a Cary 300 Bio UV-Vis spectrometer. Raman measurements for 638 and 785 nm comparison of ABTS·+ were carried out on Snowy range sierra series with 638 and 785 nm excitation wavelengths and a 3 mW (638 nm) and 4.5 mW (785 nm) power. Raman measurements for the detection of glutathione were collected using a Snowy range CBex with a 785 nm excitation wavelength and 45 mW power.

Experimental

Synthesis of Fe_2O_3 nanoparticles

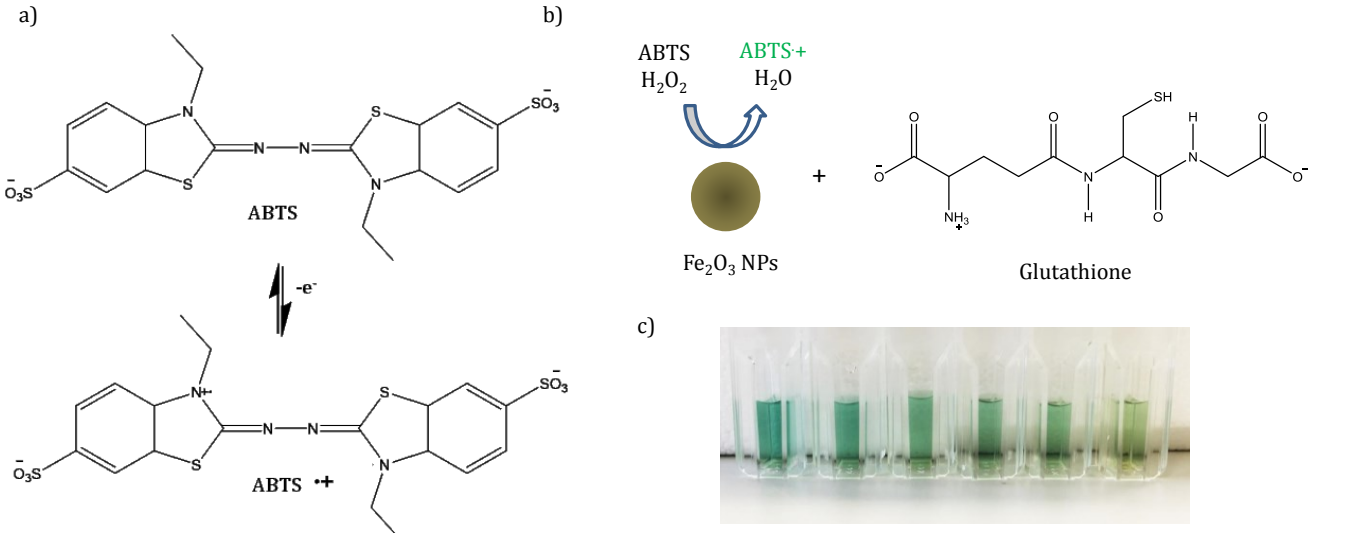

Figure 1 (a) Oxidation of ABTS to its radical cation (ABTS·+) (b) Schematic of the oxidation of ABTS decolourisation assay. Fe_2O_3 nanoparticles are used to decompose H_2O_2 initiating the oxidation of ABTS to ABTS·+. The addition of glutathione then reduces the ABTS + and the decolourisation is observed shown in (c).

Fe_2O_3 nanoparticles were synthesised using a co-precipitation method described by Donnelly *et al.*[18] $FeCl_2.4H_2O$ (1.98g),

$FeCl_3.6H_2O$ (5.335g) and HCl (821 µL) were added to 25 mL of distilled water and the solution was stirred. NaOH (15.058g) was added to a round bottom flask containing 250 mL of distilled water and heated to 50 °C. The acidified iron salt was then added dropwise to the solution with vigorous stirring for 20 mins at 50 °C and then left to settle and cool. The resulting black precipitate was washed twice with distilled water and once with 0.1 M HNO_3. 125 mL of 0.1 M HNO_3 was then added and the solution heated to 95 °C with constant stirring for 40 minutes. The resulting nanoparticles were centrifuged in triplicate and resuspended in distilled water.

Catalytic activity of Fe_2O_3 nanoparticles

200 µL of 3 mM of ABTS, 200 µL of Fe_2O_3 nanoparticles and 10 µL of 9 M H_2O_2 or 10 µL of H_2O were mixed together for 5 minutes and the nanoparticles removed with a magnet leaving the green $ABTS^{\cdot+}$ solution or colourless unoxidised ABTS solution. The solutions were then analysed using UV-vis spectroscopy by diluting 100 µL of sample with 400 µL of distilled water.

Raman analysis of $ABTS^{\cdot+}$

$ABTS^{\cdot+}$ was analysed using 638 nm and 785 nm excitation wavelengths using the same dilution used for the UV-vis spectroscopy analysis. Each spectrum was normalised against an ethanol standard taken with the same accumulation time on each instrument (1 second).

Resonance Raman detection of glutathione

Final concentrations of 0, 200, 400, 600, 1000, 1600 and 2000 nM of glutathione were added to 100 µL of $ABTS^{\cdot+}$ and the volume made up to 500 µL with distilled water. The solutions were left for 5 minutes prior to Raman measurement being taken with a 785 nm excitation wavelength at 45 mW for 1 second. The average signal intensity and standard deviation for each sample was obtained from three technical replicates with 5 acquisitions taken for each.

Resonance Raman detection of chlorogenic acid and ascorbic acid

Final concentrations of 0, 6, 12, 18 and 24 µM of chlorogenic acid or ascorbic acid were added to 100 µL of $ABTS^{\cdot+}$ and the volume made up to 500 µL with distilled water. The solutions were left for 5 minutes prior to Raman measurement being taken with a 785 nm excitation wavelength at 45 mW for 1 second. The average signal intensity and standard deviation for each sample was obtained from three technical replicates with 5 acquisitions taken for each.

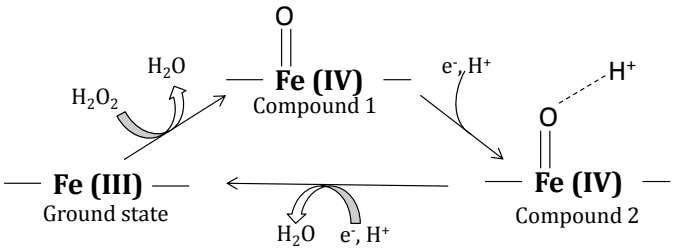

Figure 2 Reduction-Oxidation of Fe(III) by H_2O_2

Results and discussion

Traditionally, HRP has been used to catalyse the oxidation of ABTS with H_2O_2. However, it has been reported that Fe_2O_3 nanoparticles also have an intrinsic catalytic activity and they can catalyse the oxidation of ABTS in a similar manner (shown in Figure 2). When Fe_2O_3 nanoparticles are in the presence of H_2O_2, an oxygen of the H_2O_2 binds to the Fe atom initiating the reduction-oxidation of the Fe_2O_3 nanoparticles via the formation of two intermediate compounds. The Fe exists first as Fe (III) which is oxidised to Fe (IV) as the H_2O_2 is converted to water, leaving the leftover oxygen to bind to the Fe giving compound 1. An electron and H^+ ion from the ABTS then form a bond between the oxygen to form compound 2. Finally, another electron and H^+ forms water with the oxygen bonded to the Fe to allow the iron to return to Fe (III). As the Fe (IV) is reduced back to Fe(III), the ABTS is oxidised resulting in the desired coloured product.[19] The oxidation of ABTS to $ABTS^{\cdot+}$ is shown in Figure 1 (a).

Catalytic activity of Fe_2O_3 nanoparticles

Fe_2O_3 nanoparticles were synthesised using a co-precipitation method described by Donnelly *et al.*[18] In this method Fe salts were added to a base to form Fe_3O_4 nanoparticles which were then oxidised to form Fe_2O_3 nanoparticles. To demonstrate the catalytic activity of Fe_2O_3 nanoparticles, 200 µL of 3 mM of ABTS, 200 µL of Fe_2O_3 nanoparticles and 10 µL of 9 M H_2O_2 were mixed together for 5 minutes before removal of the Fe_2O_3 nanoparticles with a magnet leaving the green $ABTS^{\cdot+}$ solution behind. The solution was then characterised using UV-vis spectroscopy and the resulting spectra are shown in Figure 3 (a). The $ABTS^{\cdot+}$ has three distinct absorbance

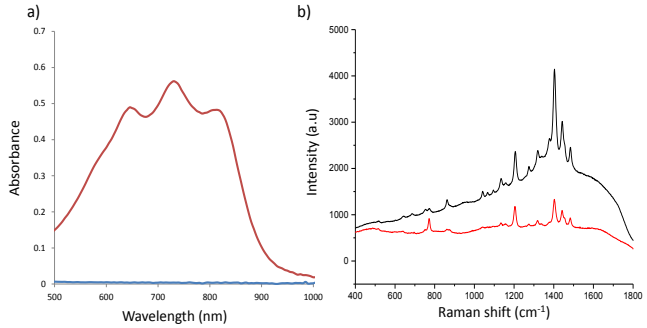

Figure 3 (a) UV-vis spectra of ABTS (blue) and $ABTS^{\cdot+}$ (red) oxidised due to the presence of Fe_2O_3 nanoparticles and H_2O_2 resulting in absorbance bands at 650, 735 and 830 nm. (b) Raman spectra of the $ABTS^{\cdot+}$ analysed using 638 nm laser excitation (red) and 785 nm laser excitation (black). Spectra were obtained using a 785 nm laser excitation with a 1 second accumulation time and 45 mW laser power and a 638 nm laser excitation with a 1 second accumulation and 30 m W laser power. The spectra shown are the average of 5 measurements of 3 replicate samples and have been normalised using an ethanol standard to take into account the relative performance of each instrument.

bands at 650 nm, 735 nm and 830 nm which only occur when Fe_2O_3 nanoparticles and H_2O_2 are both present. Control experiments were performed by replacing H_2O_2 with H_2O and demonstrated that no oxidation was experienced when a reagent was omitted; hence the Fe_2O_3 nanoparticles were only catalysing the oxidation of ABTS in the presence of H_2O_2.

Raman analysis of ABTS·+

The Raman properties of the ABTS·+ were investigated by analysing the oxidised solution with laser excitation wavelengths close to the absorbance bands at 650 nm and 735 nm as shown in the UV-vis spectrum in Figure 3 (a). Figure 3 (b) shows the Raman spectra of the ABTS·+ obtained using a 638 nm and 785 nm laser excitation which have been intensity normalised against an ethanol standard to take into account the different performance of the two different instruments which have different laser powers and excitation wavelengths. No computational calculations could be found in the literature for the assignment of the peaks in oxidised ABTS Raman spectrum, however Garcia *et al*. have used vibrational analysis of structurally related molecules to assign them[17] Table 1 lists the main characteristic peaks in the spectrum and the assignments for the peaks.

Table 1 Band assignment of ABTS·+ taken from Garcia *et al.*[17]

Peak (cm^{-1})	Assignment
1318	δ(CH); ν(CC); δ(CH3)
1439	γ(CH3); ν (CH3); ν (CC)BM

δ:In plane bending; ν:stretching; γ: out of plane; as: anti-symmetrical; BM: Benzene moiety

There are three absorbance bands present in the ABTS·+ UV-vis spectrum (Figure 3(a)) with the absorbance maximum occurring at 735 nm. Therefore it is proposed that the stronger Raman signal obtained when irradiating the radical cation with 785 nm laser excitation is due to the enhancement experienced from resonance Raman scattering. As the 785 nm laser excitation is less than 50 nm from the maximum, whilst the 638 is over 100 nm away, it is clear why the 785 nm spectrum is more enhanced compared to when 638 nm excitation is used. The lower intensity Raman spectrum obtained when excited with 638 nm laser excitation still contains the ABTS·+ characteristic peaks, however less resonance enhancement was obtained compared to 785 nm. The similarity between the two spectra and the relative intensities of the peaks in the spectra, suggest the same chromophore is being enhanced at both wavelengths but to differing degrees. Therefore 785 nm excitation was chosen for further experiments.

Resonance Raman detection of antioxidants

The decolouration ABTS assay was carried, as shown in Figure 1(b), by adding final concentrations of 0, 200, 400, 600, 1000, 1600, and 2000 nM of glutathione to the ABTS·+ solution produced from the reaction between Fe_2O_3 nanoparticles, ABTS and H_2O_2. The mixture was analysed using a portable 785 nm laser excitation instrument 5 minutes after the addition of glutathione. As higher concentrations of glutathione were added, the reduction ABTS·+ was increased which is evident due to decreasing intensity of the RRS spectra as shown in Figure 4 (a). It can be observed in Figure 4 (b) that when the intensity of the 1403 cm^{-1} peak was plotted against the glutathione concentration, a linear relationship was observed over the range of 0-2000 nM with a correlation coefficient of 0.98. The observable limit of detection was 200 nM.

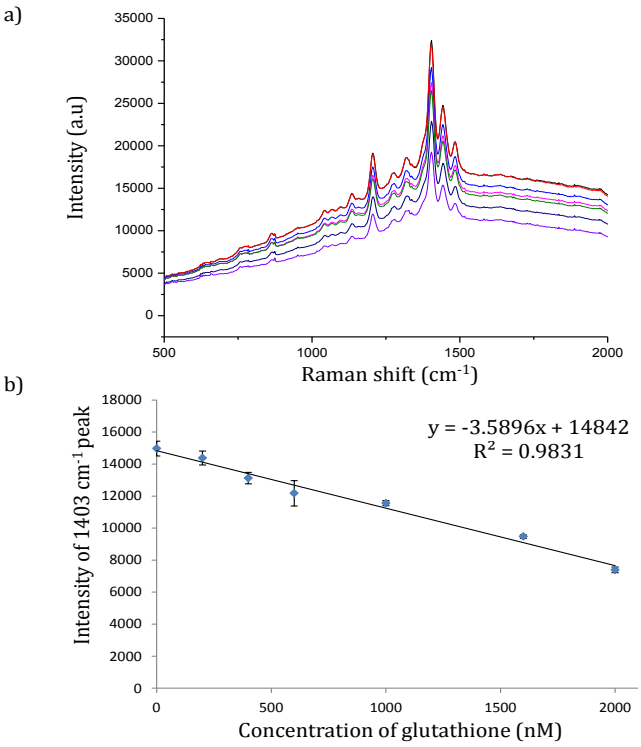

Figure 4 (a) RRS spectra of ABTS·+ obtained when different concentrations of glutathione were added (0 (black), 200 (red), 400 (light blue), 600 (pink), 1000 (green), 1600 (dark blue) and 2000 (purple) nM. (b) Plot of glutathione concentration vs peak intensity of the 1403 cm^{-1} peak of ABTS·+. The spectra were obtained using 785 nm laser excitation with a 1 second accumulation time and 45 mW laser power. Average spectra and error bars obtained from 5 measurements of 3 technical replicate samples.

The decolourisation assay was then applied for the detection of the common antioxidants chlorogenic acid (CGA), a polyphenol which has been reported to have beneficial effects for the cardiovascular and central nervous system, [20] and ascorbic acid (AA), which is vital for collagen, carnitine and neurotransmitters synthesis.[21] Final

concentrations of 0, 6, 12, 18 and 24 µM of CGA or AA were added to the ABTS·+ solution and the mixture was analysed using a portable Raman spectrometer with 785 nm laser excitation. Figure 5 shows the linear decrease in the 1403 cm^{-1} peak that occurred as higher concentrations of the antioxidants were added to the ABTS+ solution due to the reduction cause by the antioxidant. Observable detection limits of 6 µM for AA and 12 µM for CGA were obtained, indicating that the assay is versatile and can be applied for the detection of a variety of relevant antioxidants. The observable detection limits were higher than that obtained for glutathione to due to the increased reductive properties of glutathione on ABTS·+.

Using this assay, individual antioxidants would not be able to be identified however overall antioxidant activity of a sample can be measured which is invaluable information for healthcare since depleted antioxidant activity could infer oxidative stress, which can lead to a myriad of diseases.[22] The assay could also be used to detect antioxidant activity in body fluids, like plasma or urine, giving an indication of the overall antioxidant activity.

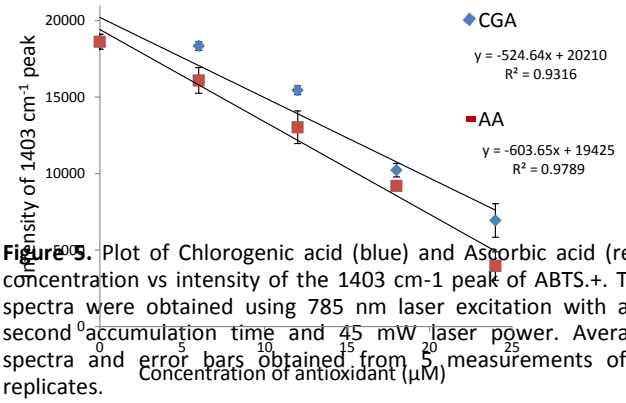

Figure 5. Plot of Chlorogenic acid (blue) and Ascorbic acid (red) concentration vs intensity of the 1403 cm-1 peak of ABTS.+. The spectra were obtained using 785 nm laser excitation with a 1 second accumulation time and 45 mW laser power. Average spectra and error bars obtained from 5 measurements of 3 replicates.

Conclusion

This work reports, to the best of our knowledge, the first use of resonance Raman detection of the ABTS decolourisation assay for the detection of glutathione. We have shown that Fe_2O_3 nanoparticles can catalyse the oxidation of ABTS with H_2O_2 yielding the green radical cation product which gives a characteristic resonance Raman spectrum when interrogated using 785 nm laser excitation. RRS was used to follow the reduction of the radical cation upon glutathione addition, leading to an observable glutathione detection limit of 200 nM. Therefore, RRS detection increased the sensitivity of the ABTS decolourisation assay, when compared to LODs obtained from the oxidation of ABTS using Fe_3O_4 NPs with UV-vis detection (3 µM),[16] ZnS quantum dots and fluorescent detection (3.3 µM) [23] and poly(caffeic acid) nanocarbon composite with electrochemical detection (0.5 µM).[24] The assay can also be used to detect the antioxidants chlorogenic and ascorbic acid with higher observable limits of detection than that of glutathione, demonstrating the versatility of the assay. Therefore the ABTS decolourisation assay using Fe_2O_3 nanoparticles and portable resonance Raman detection has led to the development of a cheap, fast, reusable assay which offers low limits of detection for various antioxidants which could be used for point of use analysis.

Acknowledgements

The authors would like to thank the EPSRC Doctoral Training Grant EP/L505080/1 and DSTL for funding. The research data associated with this paper is available at 10.15129/c34605f6-b498-4585-ae9d-b8a2c3c990ab

References

1. X. Wang, Y. Hu and H. Wei, *Inorganic Chemistry Frontiers*, 2016, **3**, 41-60.
2. L. Gao, J. Zhuang, L. Nie, J. Zhang, Y. Zhang, N. Gu, T. Wang, J. Feng, D. Yang, S. Perrett and X. Yan, *Nature nanotechnology*, 2007, **2**, 577-583.
3. K. Mitra, A. B. Ghosh, A. Sarkar, N. Saha and A. K. Dutta, *Biochemical and Biophysical Research Communications*, 2014, **451**, 30-35.
4. Q. Chang, K. Deng, L. Zhu, G. Jiang, C. Yu and H. Tang, *Microchimica Acta*, 2009, **165**, 299.
5. F. Yu, Y. Huang, A. J. Cole and V. C. Yang, *Biomaterials*, 2009, **30**, 4716-4722.
6. M.-A. Woo, M. Kim, J. Jung, K. Park, T. Seo and H. Park, *International Journal of Molecular Sciences*, 2013, **14**, 9999.
7. A. Zulueta, M. J. Esteve and A. Frígola, *Food Chemistry*, 2009, **114**, 310-316.
8. I. F. F. Benzie and J. J. Strain, *Analytical biochemistry*, 1996, **239**, 70-76.
9. M. B. Arnao, A. Cano, J. Hernández-Ruiz, F. García-Cánovas and M. Acosta, *Analytical biochemistry*, 1996, **236**, 255-261.
10. Y. Li, X. Liu and R. Zhang, *Spectrochimica Acta Part A: Molecular and Biomolecular Spectroscopy*, 2017, **173**, 880-885.
11. R. Re, N. Pellegrini, A. Proteggente, A. Pannala, M. Yang and C. Rice-Evans, *Free Radical Biology and Medicine*, 1999, **26**, 1231-1237.
12. C. D. Fernando and P. Soysa, *MethodsX*, 2015, **2**, 283-291.
13. O. Erel, *Clinical Biochemistry*, 2004, **37**, 277-285.
14. A. Pompella, A. Visvikis, A. Paolicchi, V. D. Tata and A. F. Casini, *Biochemical Pharmacology*, 2003, **66**, 1499-1503.
15. N. Ballatori, S. M. Krance, S. Notenboom, S. Shi, K. Tieu and C. L. Hammond, *Biological chemistry*, 2009, **390**, 191-214.
16. Y. Ma, Z. Zhang, C. Ren, G. Liu and X. Chen, *Analyst*, 2012, **137**, 485-489.
17. A. Garcia-Leis, D. Jancura, M. Antalik, J. V. Garcia-Ramos, S. Sanchez-Cortes and Z. Jurasekova, *Physical Chemistry Chemical Physics*, 2016, **18**, 26562-26571.
18. T. Donnelly, W. E. Smith, K. Faulds and D. Graham, *Chemical Communications*, 2014, **50**, 12907-12910.

19. G. I. Berglund, G. H. Carlsson, A. T. Smith, H. Szoke, A. Henriksen and J. Hajdu, *Nature*, 2002, **417**, 463-468.
20. K. Lee, J.-S. Lee, H.-J. Jang, S.-M. Kim, M. S. Chang, S. H. Park, K. S. Kim, J. Bae, J.-W. Park, B. Lee, H.-Y. Choi, C.-H. Jeong and Y. Bu, *European Journal of Pharmacology*, 2012, **689**, 89-95.
21. K. A. Naidu, *Nutrition Journal*, 2003, **2**, 7-7.
22. B. Uttara, A. V. Singh, P. Zamboni and R. T. Mahajan, *Current Neuropharmacology*, 2009, **7**, 65-74.
23. L. Yu, L. Li, Y. Ding and Y. Lu, *Journal of Fluorescence*, 2016, **26**, 651-660.
24. P. T. Lee, K. R. Ward, K. Tschulik, G. Chapman and R. G. Compton, *Electroanalysis*, 2014, **26**, 366-373.

